Antroquinonol displays anticancer potential against human hepatocellular carcinoma cells: A crucial role of AMPK and mTOR pathways

Po-Cheng Chiang [a], Ssu-Chia Lin [a], Shiow-Lin Pan [b], Ching-Hua Kuo [a], I-Lin Tsai [a], Mao-Tien Kuo [c], Wu-Che Wen [c], Peini Chen [d], Jih-Hwa Guh [a,e,*]

[a] School of Pharmacy, National Taiwan University, No. 1, Sect. 1, Jen-Ai Rd, Taipei 100, Taiwan
[b] Pharmacological Institute, College of Medicine, National Taiwan University, Taipei, Taiwan
[c] Golden Biotechnology Corporation, Taipei, Taiwan
[d] Taipei Veterans General Hospital, Department of Radiology, Taipei, Taiwan
[e] Division of Medicinal Chemistry, College of Pharmacy, The Ohio State University, Columbus, OH, USA

ARTICLE INFO

ABSTRACT

5′AMP-activated protein kinase (AMPK) and the mammalian target of rapamycin (mTOR) are two serine/threonine protein kinases responsible for cellular energy homeostasis and translational control, respectively. Evidence suggests that these two kniases are potential targets for cancer chemotherapy against hepatocellular carcinoma (HCC). Antroquinonol that is isolated from *Antrodia camphorate*, a well-known Traditional Chinese Medicine for treatment of liver diseases, displayed effective anticancer activity against both HBV DNA-positive and -negative HCC cell lines. The rank order of potency against HCCs is HepG2 > HepG2.2.15 > Mahlavu > PLC/PRF/5 > SK-Hep1 > Hep3B. Antroquinonol completely abolished cell-cycle progression released from double-thymidine-block synchronization and caused a subsequent apoptosis. The data were supported by down-regulation and reduced nuclear translocation of G1-regulator proteins, including cyclin D1, cyclin E, Cdk4 and Cdk2. Further analysis showed that the mRNA expressions of the G1-regulator proteins were not modified by antroquinonol, indicating an inhibition of translational but not transcriptional levels. Antroquinonol induced the assembly of tuberous sclerosis complex (TSC)-1/TSC2, leading to the blockade of cellular protein synthesis through inhibition of protein phosphorylation including mTOR (Ser^{2448}), p70^{S6K} (Thr^{421}/Ser^{424} and Thr^{389}) and 4E-BP1 (Thr^{37}/Thr^{46} and Thr^{70}). Furthermore, the AMPK activity was elevated by antroquinonol. Compound C, a selective AMPK inhibitor, significantly reversed antroquinonol-mediated effects suggesting the crucial role of AMPK. Besides, the loss of mitochondrial membrane potential and depletion of mitochondrial content indicated the mitochondrial stress caused by antroquinonol. In summary, the data suggest that antroquinonol displays anticancer activity against HCCs through AMPK activation and inhibition of mTOR translational pathway, leading to G1 arrest of the cell-cycle and subsequent cell apoptosis.

© 2009 Elsevier Inc. All rights reserved.

1. Introduction

AMP-activated protein kinase (AMPK), a serine/threonine protein kinase conserved in eukaryotes, has been proposed as a cellular energy sensor regulating the cellular adaption to environmental or nutritional stress [1]. AMPK activation leads to a decrease of energy consuming while stimulates energy production, restoring intracellular energy homeostasis. Metformin and thiazolidinedione derivatives, which were identified as AMPK activators, are clinical drugs for treatment of type II diabetes [2]. Recently, several lines of evidence suggest that AMPK can regulate cell proliferation, cell growth and autophagy [3,4]. The tumor suppressor LKB1 has been identified to activate AMPK, and another tumor suppressor, tuberous sclerosis complex 2 (TSC2), is a downstream effector of AMPK [4,5]. Furthermore, the genetic alterations of LKB1 have been suggested to play a crucial role in tumor development or progression of a sub-set of hepatocellular carcinoma (HCC) [6]. These studies provide evidence that AMPK may serve as a potential target for cancer treatment, including HCC.

The mammalian target of rapamycin (mTOR) is also a serine/threonine protein kinase that regulates cell growth by integrating nutrient- and growth factor-derived signals [7,8]. Recently, two functional complexes of mTOR have been demonstrated. One is

rapamycin-sensitive mTOR complex (mTORC1), which contains mTOR and two regulators: regulatory-associated protein of mTOR (raptor) and G protein β-subunit-like protein (GβL). The other is mTORC2, which consists of mTOR, GβL and rapamycin-insensitive companion of mTOR (rictor) [7–9]. mTORC1 regulates translation and cell growth through the phosphorylation of p70 ribosomal protein S6 kinase (p70^{S6K}) and eukaryotic initiation factor-4E (eIF4E) binding protein-1 (4E-BP1); mTORC2 is proposed to regulate PKB/AKT by the phosphorylation on Ser^{473} and plays a role on the phosphorylation of PKC-α and actin cytoskeleton [9–11]. A large body of evidence shows that rapamycin (a specific mTOR inhibitor) can inhibit the proliferation of HCC cells both in *in vitro* and *in vivo* models [12–15]. Furthermore, it has been reported that the activation of mTOR pathways occurs in about 50% of patients with HCC [16]. One important issue for the therapeutic treatment of HCC is the resistance problem. The resistance to apoptosis induced by chemotherapeutic drugs enables the neoplastic cells to survive. More recently, the regulation of resistance mechanism by mTOR pathways has been investigated and the studies demonstrate that the inhibition of mTOR pathways can sensitize apoptosis induced by chemotherapeutic drugs in HCC [17].

Antrodia camphorata, a camphor tree mushroom, is a precious traditional Chinese herbal medicine and shows several pharmacological effects including the inhibition of proliferation and growth in cancer cells [18–20], the inhibition of inflammatory response [21], the antioxidant and free radical-scavenging activities [22,23] and the prevention of hepatotoxicity [23]. *Antrodia camphorata* is rich in flavonoids, terpenoids, polyphenolics and polysaccharides. In this study, we have characterized the anticancer effect of antroquinonol, a new component from *Antrodia camphorate* [24]. We found that antroquinonol potently inhibited the proliferation and growth of several HCC cell lines. The mechanism of action has been studied and the data reveal the involvement of AMPK and mTOR translational signaling pathways. To our knowledge, this study is the first report that demonstrates the crucial roles of AMPK and mTOR pathways on the anticancer effect induced by *Antrodia camphorate* components.

2. Materials and methods

2.1. Materials

Dulbecco's Modified Eagle Medium (DMEM), fetal bovine serum (FBS), penicillin, streptomycin, and all other tissue culture regents were obtained from GIBCO/BRL Life Technologies (Grand Island, NY). Antibodies to GAPDH, cyclin D1, cyclin E, cyclin-dependent kinase 4 (Cdk4), Cdk2, nucleolin and anti-mouse and anti-rabbit IgGs were obtained from Santa Cruz Biotechnology, Inc. (Santa Cruz, CA). Antibodies to p53, p53^{Ser15}, 4E-BP1, phospho-4E-BP1$^{Thr37/Thr46}$, phospho-4E-BP1^{Thr70}, p70S6K, phospho-p70S6K$^{Thr421/Ser424}$, phosphor-p70S6K^{Thr389}, AMPKα, phospho-AMPKα^{Thr172}, Akt^{Ser473}, Erk1/2, Erk1/2$^{Thr202/Tyr204}$ and α-tubulin were from Cell Signaling Technologies (Boston, MA). Sulforhodamine B (SRB), propidium iodide (PI), phenylmethylsulfonylfluoride (PMSF), leupeptin, dithiothreitol (DTT), rhodamine 123, EDTA, Compound C (6-[4-(2-Piperidin-1-ylethoxy)phenyl]-3-pyridin-4-ylpyrazolo[1,5-a]pyrimidine), trichloroacetic acid (TCA), citric acid, Triton X-100, RNase, aprotinin, sodium orthovanadate, ethidium bromide, glutaraldehyde, osmic acid, uranyl acetate, lead citrate, β-glycerophosphate and all of the other chemical reagents were obtained from Sigma–Aldrich (St. Louis, MO). Antroquinonol was purified from *Antrodia camphorate*. The purification and structure identification of antroquinonol were demonstrated elsewhere [24].

2.2. Cell lines and cell culture

The cancer cell lines including HepG2, PLC/PRF/5 and Hep3B were from American Type Culture Collection (Rockville, MD). The other cell lines were obtained from Hepatitis Research Center, National Taiwan University Hospital. The cells were cultured in DMEM medium with 10% FBS (v/v) and penicillin (100 units/ml)/streptomycin (100 μg/ml). Cultures were maintained in a humidified incubator at 37 °C in 5% CO_2/95% air.

2.3. SRB assays

Cells were seeded in 96-well plates in medium with 5% FBS. After 24 h, cells were fixed with 10% TCA to represent cell population at the time of compound addition (T_0). After additional incubation of DMSO or antroquinonol for 48 h, cells were fixed with 10% TCA and SRB at 0.4% (w/v) in 1% acetic acid was added to stain cells. Unbound SRB was washed out by 1% acetic acid and SRB bound cells were solubilized with 10 mM Trizma base. The absorbance was read at a wavelength of 515 nm. Using the following absorbance measurements, such as time zero (T_0), control growth (C), and cell growth in the presence of the compound (Tx), the percentage growth was calculated at each of the compound concentrations levels. Percentage growth inhibition was calculated as: $100 - [(Tx - T_0)/(C - T_0)] \times 100$. Growth inhibition of 50% (IC_{50}) is determined at the compound concentration which results in 50% reduction of total protein increase in control cells during the compound incubation.

2.4. Cell-cycle synchronization

Synchronization of HepG2 cells was performed by double thymidine block. Briefly, cells were treated with 3 mM thymidine in medium/10% FCS for 16 h and washed twice with PBS and then cultured in fresh medium/10% FCS for 10 h. The cells were treated again with medium/10% FCS containing 3 mM thymidine for 16 h. After washing cells with PBS, the block was released by the incubation of cells in fresh medium/10% FCS (indicated as time zero), and cells were harvested at 0, 3, 6, 9, 12 and 18 h. The cell-cycle progression was detected by flow cytometric analysis.

2.5. FACScan flow cytometric assay

After the treatment of cells with vehicle (0.1% DMSO) or antroquinonol for the indicated times, the cells were harvested by trypsinization, fixed with 70% (v/v) alcohol at 4 °C for 30 min and washed with PBS. After centrifugation, cells were incubated in 0.1 ml of phosphate–citric acid buffer (0.2 M NaHPO$_4$, 0.1 M citric acid, pH7.8) for 30 min at room temperature. Then, the cells were centrifuged and resuspended with 0.5 ml PI solution containing Triton X-100 (0.1% v/v), RNase (100 μg/ml) and PI (80 μg/ml). DNA content was analyzed with FACScan and CellQuest software (Becton Dickinson, Mountain View, CA).

2.6. Nuclear extraction

To prepare nuclear extracts, total cell lysates were resuspended in buffer A containing 10 mM HEPES (pH 7.9), 1.5 mM MgCl$_2$, 10 mM KCl, 0.5 mM DTT, and 0.2 mM PMSF, and kept at 4 °C for 10 min. The samples were centrifuged at 2000 rpm for 2 min. The nuclear pellets were further resuspended in ice-cold buffer C containing 20 mM HEPES (pH 7.9), 25% (v/v) glycerol, 420 mM NaCl, 1.5 mM MgCl$_2$, 0.2 mM EDTA, 0.5 mM DTT, and 0.2 mM PMSF for 20 min, and centrifuged at 15,000 rpm for 2 min. Supernatants containing the solubilized nuclear proteins were used for Western blotting.

2.7. Western blotting

After the treatment, cells were harvested with trypsinization, centrifuged and lysed in 0.1 ml of lysis buffer containing 10 mM Tris–HCl (pH 7.4), 150 mM NaCl, 1 mM EGTA, 1% Triton X-100, 1 mM PMSF, 10 μg/ml leupeptin, 10 μg/ml aprotinin, 50 mM NaF and 100 μM sodium orthovanadate. Total protein was quantified, mixed with sample buffer and boiled at 90 °C for 5 min. Equal amount of protein (30 μg) was separated by electrophoresis in 8 or 12% SDS-PAGE, transferred to PVDF membranes and detected with specific antibodies. The immunoreactive proteins after incubation with appropriately labeled secondary antibody were detected with an enhanced chemiluminescence detection kit (Amersham, Buckinghamshire, UK).

2.8. RNA extraction and reverse transcription polymerase chain reaction (RT-PCR)

Total RNA was extracted (20 μg). The PCR primers pairs used for genes amplification were demonstrated in Table 1. After denaturation at 94 °C for 2 min, PCR was performed in a Robocycler Gradient 96 (Stratagene) for 30 cycles. Each reaction cycle includes denaturation at 94 °C for 1 min, annealing at 55 °C for 1 min, and extension at 72 °C for 1 min, followed by a final extension at 72 °C for 10 min. PCR products were analyzed on 1.5% agarose gel in TAE buffer (40 mM Tris acetate, 1 mM EDTA), and visualized in the presence of 1 μg/ml ethidium bromide staining using BioDoc-It Imaging System (UVP, Upland, CA, USA).

Table 1
Primers used for RT-PCR experiments.

Gene	Primers	Base pair
Cyclin D1	Fw 5′-CGG AGG AGA ACA AAC AGA TC-3′ Rev 5′-GGG TGT GCA AGC CAG GTC CA-3′	350 bp
Cyclin E	Fw 5′-TCC TCA CCC CGC CAC AGA GC-3′ Rev 5′-CAG CAT CGG GAG CAC GCA CT-3′	307 bp
Cdk4	Fw 5′-CTT TGA CCT GAT TGG GCT GC-3′ Rev 5′-GGA GAG GTG GGA GGG GAA TG-3′	396 bp
Cdk2	Fw 5′-TTT GGA GTC CCT GTT CGT AC-3′ Rev 5′-TGC GAT AAC AAG CTC CGT CC-3′	341 bp
GAPDH	Fw 5′-TCC TTG GAG GCC ATG TGG GCC AT-3′ Rev 5′-TGA TGA CAT CAA GAA GGT GGT GAA G-3′	240 bp

2.9. Measurement of mitochondrial membrane potential ($\Delta\Psi_m$)

Cells were treated with or without antroquinonol. Thirty minutes before the termination of incubation, a rhodamine 123 solution (final concentration of 5 μM) was added to the cells and incubated for the last 30 min at 37 °C. The cells were finally harvested and the accumulation of rhodamine 123 was determined using FACScan flow cytometric analysis.
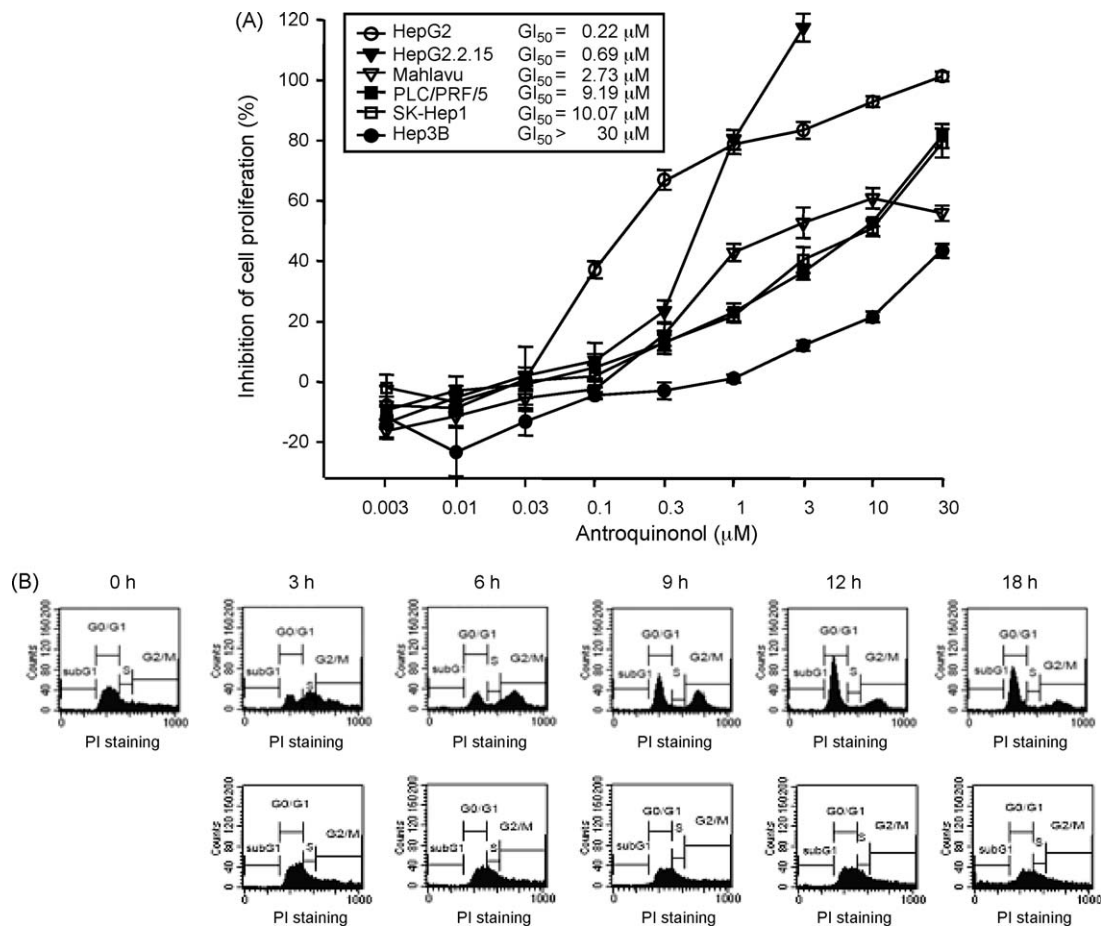
Fig. 1. (A) Identification of anti-proliferative effect of antroquinonol. The graded concentrations of antroquinonol were added to cells for 48 h. Then, cells were fixed and stained with SRB. After a series of washing, bound SRB was subsequently solubilized and the absorbance was read at a wavelength of 515 nm. Data are expressed as mean ± SEM of three to five determinations (each in triplicate). (B) Effect of antroquinonol on cell-cycle progression. Synchronization of HepG2 cells was performed by double thymidine block as described in Section 2. Then, the cells were released in the absence (upper panel) or presence of 3 μM antroquinonol (lower panel). Data are representative of two independent experiments.

2.10. Electron microscopic examination

Cells were washed twice with PBS and fixed with 2% glutaraldehyde, and then in 1% osmic acid/0.1 M cacodylate buffer. Samples were dehydrated in a series of alcohols and embedded in Epon 812 by standard procedures. Ultra-thin sections were prepared, stained with both uranyl acetate and lead citrate, and assessed using a Hitachi 7100 electron microscope.

2.11. Immunoprecipitation assay

After treatment with vehicle or the indicated agent, the cells were washed twice with ice-cold PBS, lysed in 700 ml of lysis buffer containing 20 mM Tris, pH 7.5, 1 mM $MgCl_2$, 125 mM NaCl, 1% Triton X-100, 1 mM PMSF, 10 μg/ml leupeptin, 10 μg/ml aprotinin, 25 mM β-glycerophosphate, 50 mM NaF, and 100 μM sodium orthovanadate, and centrifuged. The supernatant was immunoprecipitated with the antibody against TSC2 in the presence of A/G-agarose beads overnight. The beads were washed four times with lysis buffer for immunoblotting.

2.12. [³H]leucine incorporation assay

The protein synthesis of cells was measured by quantitating [³H]leucine incorporation. Briefly, cells were seeded into each well of 96-well culture plates. After 24 h, the cells were incubated in medium containing [³H]leucine (2 μCi/ml, Amersham) and then treated with or without antroquinonol for the indicated times at 37 °C. After the treatment, the cells were harvested using a filter mate micro-harvester (PerkinElmer Life and Analytical Sciences, Boston, MA) and incorporated radioactivity was determined.

2.13. Data analysis

The compound was dissolved in DMSO. The final concentration of DMSO was 0.1% in cell culture media. Data are presented as the mean ± SEM for the indicated number of separate experiments. Statistical analysis of data was performed with one-way analysis of variance (ANOVA) followed by a t-test and p-values less than 0.05 were considered significant.
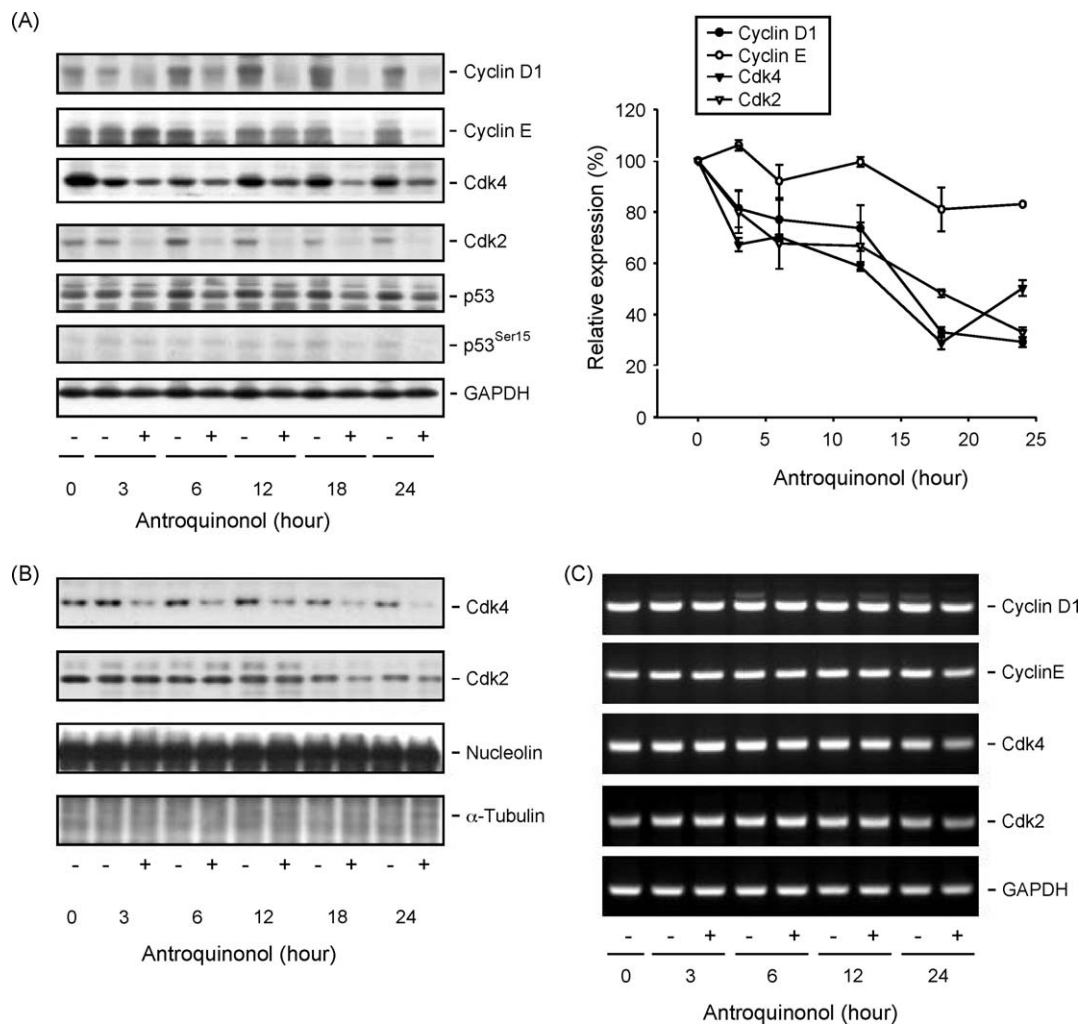
Fig. 2. (A) Effect of antroquinonol on expressions of cell-cycle regulators. HepG2 cells were incubated in the absence or presence of antroquinonol (3 μM) for the indicated times. Then, the cells were harvested and lysed for the detection of the indicated protein expressions by Western blot. The expressions were quantified using the computerized image analysis system ImageQuant (Amersham Biosciences). The data are expressed as mean ± SEM of two to three independent experiments. (B) Determination of nuclear translocation of Cdk4 and Cdk2. HepG2 cells were incubated in the absence or presence of antroquinonol (3 μM) for the indicated times. Then, the cells were harvested for the preparation of nuclear extracts and the detection of protein expression by Western blotting as described in Section 2. The nuclear extracts were verified by positive staining of nucleolin while negative to α-tubulin. (C) Determination of mRNA levels. HepG2 cells were incubated in the absence or presence of antroquinonol (3 μM) for the indicated times. Then, the cells were harvested for the determination of mRNA expression by RT-PCR.

3. Results

3.1. Anti-proliferative activity in HCC cell lines

Several HCC cell lines were used to examine the anti-proliferative effect of antroquinonol. PLC/PRF/5 and Hep3B are hepatitis B virus (HBV) DNA-positive cells. HepG2.2.15 cells, a subline of HepG2, are stably transfected with a complete HBV genome, producing viral genomes and secreting virus-like particles. HepG2, Mahlavu and SK-Hep1 are negative for HBV sequences. The data demonstrated that antroquinonol was effective in all tested cell lines and HepG2 cells were the most susceptible to the anti-proliferative effect (Fig. 1A). To detect the cell-cycle progression, HepG2 cells were synchronized at G1/S phase by using double thymidine block. Upon release from the block, more than 80% of the cells progressed into S and G2/M

phases (0–6 h). In the presence of antroquinonol (3 μM), the cell-cycle progression was almost completely blocked and the population of apoptotic cells increased after an 18-h release from double thymidine block (Fig. 1B).

3.2. Effect of antroquinonol on expressions of cell-cycle regulators

The cell-cycle progression is regulated by periodic activation of various Cdk/cyclin complexes. Cyclin D1 and its catalytic partner Cdk4 dominate G1 phase. Cyclin E/Cdk2 complex regulates the cell-cycle progression from G1 to S. Antroquinonol induced a time-related decrease of protein level of these regulators (Fig. 2A). Additionally, the expression of p53 was down-regulated after the exposure to antroquinonol for 18 h (Fig. 2A). The detection of nucleus fraction-associated proteins showed that antroquinonol reduced the nuclear translocation of
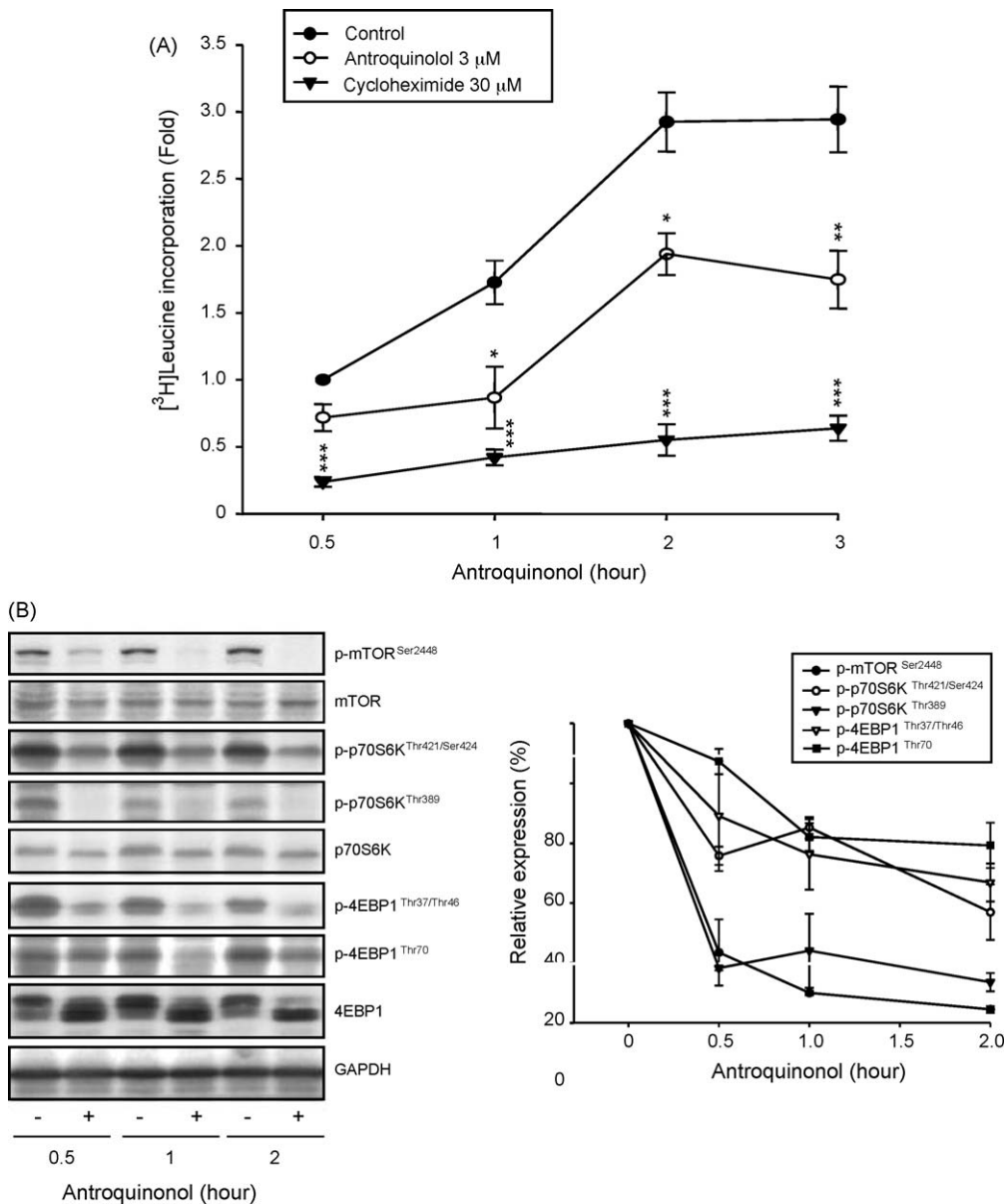
Fig. 3. (A) Effect of antroquinonol on cellular protein synthesis. HepG2 cells were treated without (control) or with antroquinonol or cycloheximide for the indicated times. After the treatment, the protein synthesis was examined by [^{3}H]leucine incorporation assay. Data are expressed as mean ± SEM of three determinations (each in triplicate). $^*P < 0.05$, $^{**}P < 0.01$ and $^{***}P < 0.001$ compared with the respective control. (B) Effect of antroquinonol on translational signaling. HepG2 cells were treated with or without antroquinonol (3 μM) for 0.5, 1 and 2 h. Then, the cells were harvested and lysed for the detection of the indicated protein expressions by Western blot. The expressions were quantified using the computerized image analysis system ImageQuant (Amersham Biosciences). Data are expressed as mean ± SEM of two determinations.
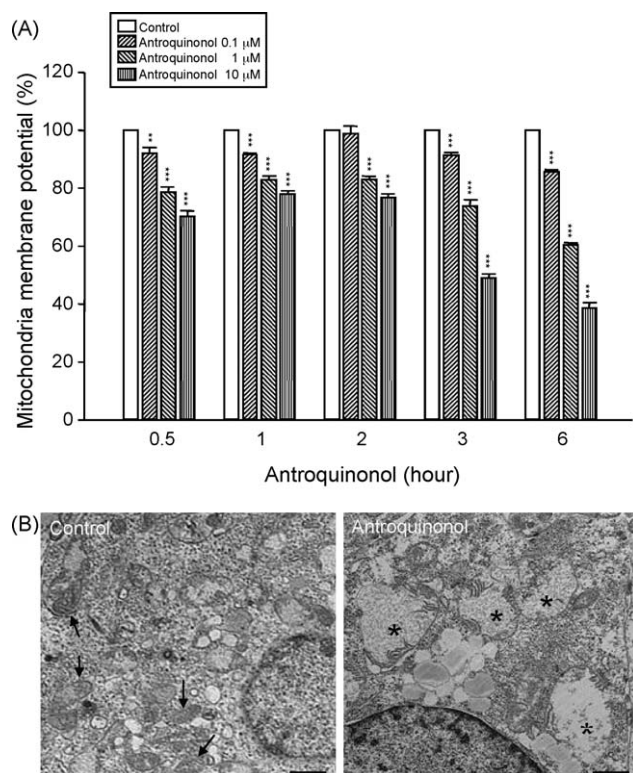
Fig. 4. (A) Effect of antroquinonol on $\Delta\Psi_m$. HepG2 cells were treated without (control) or with antroquinonol for the indicated times. The cells were incubated with rhodamine 123 for the detection of $\Delta\Psi_m$ using FACScan flow cytometric analysis. Data are expressed as mean ± SEM of three independent determinations. [**]$P < 0.01$ and [***]$P < 0.001$ compared with the respective control. (B) Effect of antroquinonol on mitochondrial content. HepG2 cells were incubated in the absence (control) or presence of antroquinonol (3 μM) for 10 h. After a series of washing, fixation and dehydration, ultra-thin sections of samples were prepared and stained for the assessment using an electron microscope. The ultrastructural morphology of mitochondria was observed. Normal mitochondria were observed in control cells (arrow); whereas, the depletion of mitochondrial content and the fusion of empty content (star) were detected in cells responsive to antroquinonol. Scale bar, 1 μm.

Cdk4 and Cdk2 as well (Fig. 2B). RT-PCR analysis revealed that the mRNA levels of G1-S regulators remained constant except for a long-term treatment (24 h), indicating that antroquinonol did not regulate the transcriptional levels of the cell-cycle regulators (Fig. 2C).

3.3. Regulation of translational pathways and protein synthesis

Cellular protein synthesis allows cell growth and, in turn, cell-cycle progression. The rate of protein synthesis contributes essentially to the lengths of G1 phase [25]. The cellular protein synthesis was determined by [³H]leucine incorporation assay and the data showed that both antroquinonol and cycloheximide, a protein synthesis inhibitor, caused a rapid and significant block of cellular protein synthesis in HepG2 cells (Fig. 3A). Accordingly, the signals responsible for translational control were examined. Antroquinonol dramatically inhibited the phosphorylation of mTOR at Ser^{2448}, $p70^{S6K}$ at Thr^{421}/Ser^{424} and Thr^{389} and 4E-BP1 at Thr^{37}/Thr^{46} and Thr^{70} (Fig. 3B). The data suggest that antroquinonol induces an inhibitory effect on mTOR-mediated translational pathways.

3.4. Mitochondrial function and $\Delta\Psi_m$

Mitochondrial function is critical to cell viability. The loss of mitochondrial function results in a lack of oxidative ATP generating

capacity. Protein synthesis at G1 phase is susceptible to mitochondrial dysfunction, leading to G1 checkpoint arrest and cell apoptosis [26,27]. The data demonstrated that antroquinonol caused a time- and concentration-dependent loss of $\Delta\Psi_m$ (Fig. 4A). The electron microscopic examination also showed the depletion of mitochondrial content and the fusion of empty content in HepG2 cells responsive to antroquinonol (Fig. 4B).

### 3.5. Upstream signals of translational regulation

Numerous molecular signals have been suggested to regulate translational signaling pathways. The activation of Akt and MAPK pathways may link mTOR-mediated translational signaling [7,10,11,28]. Additionally, AMPK plays a key role in connecting cellular energy homeostasis and protein synthesis [4,29]. The Western blot analysis showed that antroquinonol had little effect on Akt and p38 MAPK activity by detection of kinase phosphorylation (Fig. 5A). However, AMPK activity was significantly induced by antroquinonol (Fig. 5A) and the onset of kinase activity was comparable to the effect on mitochondrial dysfunction. Additionally, Compound C (a selective and ATP-competitive inhibitor of AMPK) significantly impeded antroquinonol-induced loss of $\Delta\Psi_m$ although Compound, by itself, caused a modest effect (15%) on mitochondrial function at high concentration (Fig. 5B). Moreover, the Western blot analysis demonstrated that Compound C rescued the antroquinonol-mediated inhibitory effect on $p70^{S6K}$ phosphorylation and 4E-BP1 phosphorylation (Fig. 5C).

3.6. Regulation of Erk1/2 phosphorylation and assembly of TSC2/TSC1 complex

One particular effect of HepG2 cells in response to antroquinonol was the stimulation of Erk1/2 activation (Fig. 6A). It has been suggested that Erk1/2 activation, contrary to AMPK stimulation, may cause TSC1–TSC2 dissociation and impair TSC2 capability of blocking mTOR signaling [30]. In this study, the immunoprecipitation assay showed that antroquinonol stimulated an increase of TSC1/TSC2 association, which was significantly inhibited by Compound C, indicating that AMPK overrode Erk1/2 and promoted the TSC1/TSC2 assembly (Fig. 6B). Furthermore, Compound C did not block antroquinonol-mediated Erk activation; on the contrary, the Erk activity was moderately increased (Erk1, 51%; Erk2, 28%) under the blockade of AMPK activity (Fig. 6C).

4. Discussion

Antrodia camphorata is a basidiomycete and is well known as a Traditional Chinese Medicine for the treatment of liver diseases. Antroquinonol, a component purified from *Antrodia camphorate* displayed effective anticancer activity against both HBV DNA-positive and -negative HCC cell lines. The most susceptible cell line, HepG2, was selected for the study of mechanism of action. In G1 phase of the cell-cycle, cyclin D1 and its cognate Cdk (Cdk4/6) are responsible for transition to S phase by phosphorylating retinoblastoma gene (pRB). The aberrations of Cdk4 and cyclin D1 genes have been suggested to involve in oncogenesis. Furthermore, the cyclin D1 gene was amplified in patients at an advanced stage of HCC with rapid tumor growth [31]. These studies suggest that the amplification and overexpression of cyclin D1 and Cdk4 genes may lead to the rapid growth of HCC. Antroquinonol caused a down-regulation of G1 cyclins and Cdks, leading to G1 arrest of the cell-cycle and a subsequent cell death. This effect may be of potential to the subset of HCC that has amplified and overexpressed G1 cyclins and Cdks. However, our data also showed that HBV DNA-positive cell lines were less susceptible to antroquinonol action. It has been suggested that hepatitis B virus X protein (HBx) is able to induce
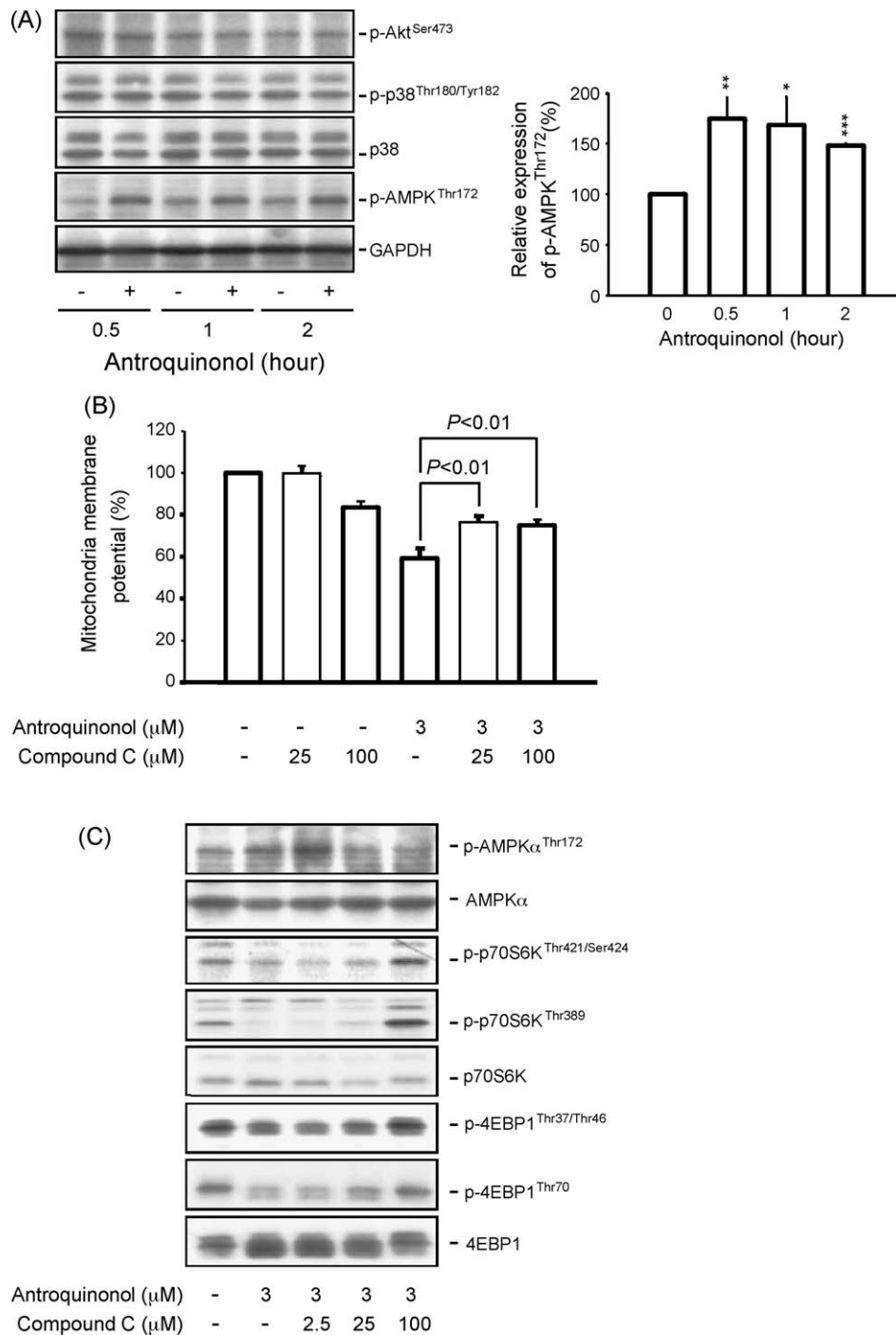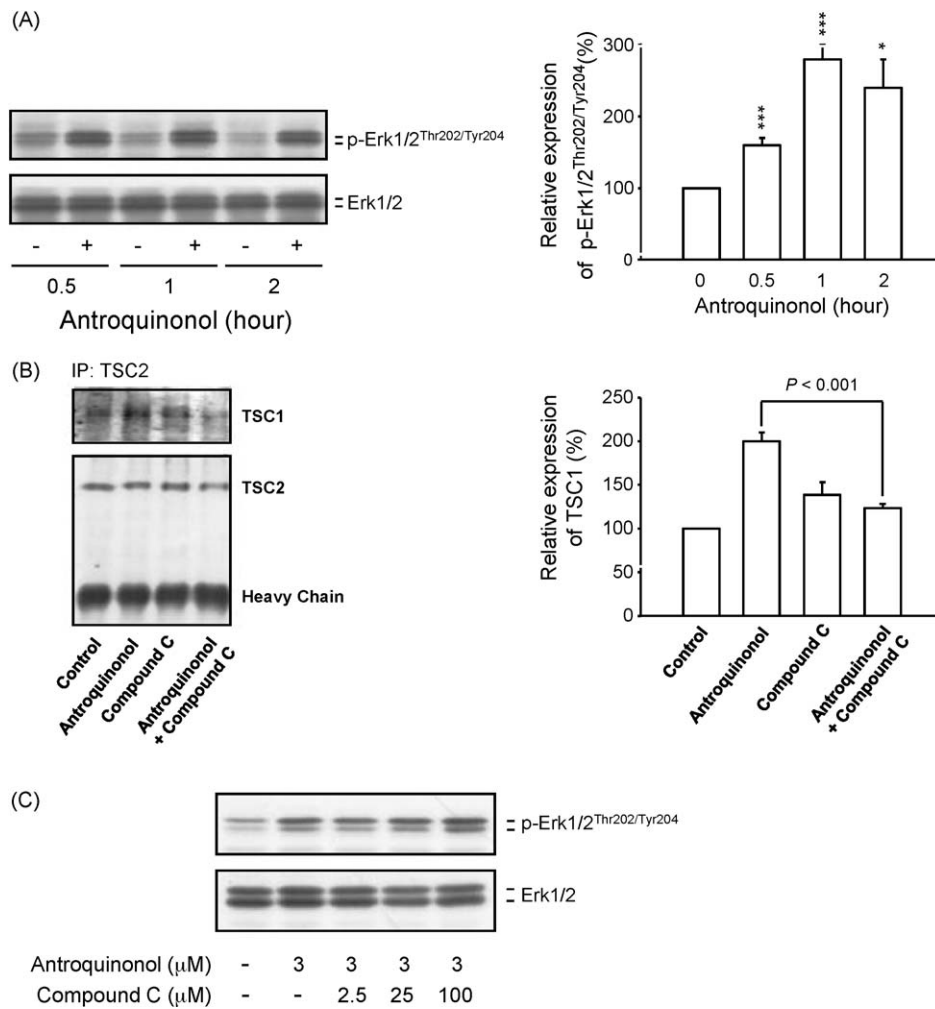
Fig. 5. (A) Effect of antroquinonol on expressions of several proteins. HepG2 cells were incubated in the absence or presence of antroquinonol (3 μM) for 0.5, 1 and 2 h. Then, the cells were harvested and lysed for the detection of the indicated protein expressions by Western blot. The expressions were quantified using the computerized image analysis system ImageQuant (Amersham Biosciences). The data are expressed as mean ± SEM of three independent experiments. $^*P < 0.05$, $^{**}P < 0.01$ and $^{***}P < 0.001$ compared with the control. (B) Effect of Compound C on the restoration of $\Delta\Psi_m$. HepG2 cells were treated without or with antroquinonol or Compound C for 3 h. The cells were incubated with rhodamine 123 for the detection of $\Delta\Psi_m$ using FACScan flow cytometric analysis. Data are expressed as mean ± SEM of three independent determinations. (C) Effect of Compound C on the restoration of protein expression. HepG2 cells were treated without or with antroquinonol or Compound C for 1 h. Then, the cells were harvested and lysed for the detection of the indicated protein expressions by Western blot.

cyclin D1 up-regulation and activate DNA methyltransferase 1 expression, which is associated with increased cell proliferation and is considered to play an essential role in aberrant DNA methylation in tumors [32,33]. The HBx-elicited effect, which was contrary to antroquinonol action, might partly explain the resistant outcome.

The protein synthesis and degradation are two major processes that regulate the levels of protein expressions. In our unshown data, antroquinonol did not modify the protein degradation. In contrast, it significantly inhibited the protein synthesis by [3H]leucine incorporation assay. The data also showed that antroquinonol considerably reduced the phosphorylation of p70^{S6K} at Thr^{389} and Thr^{421}/Ser^{424}. The phosphorylation of Thr^{389} in the catalytic domain most closely correlates with p70^{S6K} kinase activity [34]. Phosphorylation at Thr^{421} and Ser^{424}, which locate in pseudosubstrate region of p70^{S6K}, can activate the

(A)

(B)

(C)

Fig. 6. (A) Effect of antroquinonol on Erk phosphorylation. HepG2 cells were incubated in the absence or presence of antroquinonol (3 μM) for 0.5, 1 and 2 h. Then, the cells were harvested and lysed for the detection of the indicated protein expressions by Western blot. The expressions were quantified using the computerized image analysis system ImageQuant (Amersham Biosciences). The data are expressed as mean ± SEM of two independent experiments. $*P < 0.05$ and $***P < 0.001$ compared with the control. (B) Determination of TSC1–TSC2 association. HepG2 cells were treated without or with antroquinonol (3 μM) or Compound C (100 μM) for 2 h. Then, the cells were harvested for the immunoprecipitation assay as described in Section 2. The expressions were quantified using the computerized image analysis system ImageQuant (Amersham Biosciences). Data are expressed as mean ± SEM of two determinations. (C) Effect of Compound C on antroquinonol-induced Erk phosphorylation. HepG2 cells were treated without or with antroquinonol or Compound C for 2 h. Then, the cells were harvested and lysed for the detection of the indicated protein expressions by Western blot.

kinase through relief of pseudosubstrate suppression [35]. The data indicate that antroquinonol induce an inhibitory effect on p70[S6K] activity. Besides, it has been identified that p70[S6K] activity remains high throughout G1 phase and is essential for G1 progression [35,36]. These studies further support that antroquinonol induces G1 arrest in HepG2 cells. 4E-BP1, a translation repressor protein, inhibits cap-dependent translation by binding to translation initiation factor eIF4E. Hyperphosphorylation of 4E-BP1 interrupts this association, leading to activation of cap-dependent translation [37]. Similarly, 4E-BP1 phosphorylation was inhibited by antroquinonol that could restore the interaction between 4E-BP1 and eIF4E and halt the subsequent translational cascades.

Currently, the target on mTOR signaling pathways is extensively investigated for cancer chemotherapy including HCC. The rationale is supported by the evidence that the mTOR pathway is activated in near 50% of patients with HCC [16] and mTOR inhibitors are effective in reducing tumor mass and vasculature [15,38]. The prototypic mechanism that regulates mTOR signaling is through the activation of phosphatidyl inositol-3 kinase (PI3K)/Akt pathway [7,10], but mTOR also receives signals from pathways that are PI3K/Akt-independent, such as Erk, p38 MAPK and AMPK [39,40]. First, we identified the

possible upstream kinases, Akt and p38 MAPK. The data showed that antroquinonol caused translational inhibition neither through blockade of PI3K/Akt pathway nor via modification of p38 MAPK activity.

AMPK is a heterotrimeric complex composed of a catalytic α subunit and regulatory β and γ subunits. AMPK is activated under conditions that deplete ATP and elevate AMP levels such as hypoxia, ischemia, heat shock and glucose deprivation that caused an elevated AMP/ATP ratio [1,41]. Recently, AMPK activation by the activator, AMP-mimetic 5-aminoimidazole-4-carboxamide ribonucleoside (AICAR), has been demonstrated to induce cell-cycle arrest in HepG2 cells. These reports suggest that p53 accumulation and phosphorylation at Ser^{15} explain part of the arrest mechanism [42]. In this study, antroquinonol induced a significant increase of AMPK activity within a 30-min treatment, indicating that AMPK served as an upstream effector to antroquinonol action. However, p53 was not responsible for the cell-cycle arrest since there were no apparent p53 up-regulation and phosphorylation. There is increasing evidence that AMPK communicates the cellular energy status to mTOR pathway. In the absence of cell growth stimuli, TSC2 associates with TSC1 to form a complex that inhibits protein synthesis and cell growth via repression of mTOR [39]. Upon the mitogenic stimuli, TSC2 is phosphorylated at Ser^{939} and Thr^{1462}

that cause the inhibition of TSC2, leading to the activation of mTOR pathway [39,43]. Antroquinonol induced the activation of AMPK that, in turn, blocked mTOR pathway as revealed by the inhibition of phosphorylation of p70[S6K] and 4E-BP1, and the increased association of TSC1 and TSC2. The data were further supported by the evidence that Compound C (a selective AMPK inhibitor) effectively rescued the phosphorylation of both p70[S6K] and 4E-BP1. However, 100 μM Compound C, by itself, induced a moderate increase of phosphorylated p70S6K and 4E-BP1 (data not shown). This stimulatory effect may, at least partly, explain the rescue consequence of Compound C.

Recently, the regulation of TSC2 by Erk pathway has been reported. The activated Erk phosphorylates TSC2 at Ser[540] and Ser[664] that induce the dissociation of TSC1/TSC2 complex and reduction of TSC2 activity, leading to the activation of mTOR signaling [30]. Similarly, our study demonstrated that antroquinonol not only activated AMPK but also induced the activation of Erk1 and Erk2. However, the ultimate effect on mTOR signaling and cell-cycle progression favored to AMPK-mediated inhibitory pathways. The data were consistent with the report by Nagata and the colleagues that AMPK activation can overcome growth signaling from mitogenic stimuli and can maintain cells in a quiescent state similar to G0 phase [44]. Moreover, antroquinonol-mediated Erk activation was modestly elevated in the condition of AMPK blockade by Compound C indicating a crosstalk between Erk and AMPK activity. Finally, we tried to identify the mechanism underlying the AMPK activation by antroquinonol. There is increasing evidence that the stress on mitochondria induced by hormones, cytokines and pharmacological agents may lead to AMPK activation in many cell types [45]. The mitochondrial function was determined and the data showed that antroquinonol induced the loss of $\Delta\Psi_m$ that was correlated to the time frame of AMPK activation. Notably, Compound C significantly protected the mitochondrial function by 43%, suggesting that AMPK activation might further exacerbate the mitochondrial function.

As for the in vivo efficacy, because the take rate of HepG2 xenografts is limited to less than 30%, we performed the in vivo study using Hep3B derived cancer xenografts. In our unshown data, antroquinonol (50 mg/kg, i.p.) prolonged the doubling time of the tumor from 4 days to 12 days, indicating that antroquinonol is in vivo active.

Taken together, the data suggest that antroquinonol induces anticancer signaling cascades in a sequential manner. The exposure of cells to antroquinonol induces mitochondrial stress and activation of AMPK that further induces the loss of $\Delta\Psi_m$ and activates TSC1/TSC2 association. Consequently, the mTOR-mediated translational pathways are blocked, leading to G1 arrest of the cell-cycle and subsequent cell death.

Acknowledgements

Appendix A. Supplementary data

Supplementary data associated with this article can be found, in the online version, at doi:10.1016/j.bcp.2009.08.022.

References

[1] Koh HJ, Brandauer J, Goodyear LJ. LKB1 and AMPK and the regulation of skeletal muscle metabolism. Curr Opin Clin Nutr Metab Care 2008;11:227–32.
[2] Mauvais-Jarvis F, Andreelli F, Hanaire-Broutin H, Charbonnel B, Girard J. Therapeutic perspectives for type 2 diabetes mellitus: molecular and clinical insights. Diabetes Metab 2001;27:415–23.
[3] Høyer-Hansen M, Jäättelä M. AMP-activated protein kinase: a universal regulator of autophagy? Autophagy 2007;3:381–3.
[4] Luo Z, Saha AK, Xiang X, Ruderman NB. AMPK, the metabolic syndrome and cancer. Trends Pharmacol Sci 2005;26:69–76.
[5] Mak BC, Yeung RS. The tuberous sclerosis complex genes in tumor development. Cancer Invest 2004;22:588–603.
[6] Kim CJ, Cho YG, Park JY, Kim TY, Lee JH, Kim HS, et al. Genetic analysis of the LKB1/STK11 gene in hepatocellular carcinomas. Eur J Cancer 2004;40:136–41.
[7] Fingar DC, Blenis J. Target of rapamycin (TOR): an integrator of nutrient and growth factor signals and coordinator of cell growth and cell cycle progression. Oncogene 2004;23:3151–71.
[8] Dann SG, Thomas G. The amino acid sensitive TOR pathway from yeast to mammals. FEBS Lett 2006;580:2821–9.
[9] Sarbassov DD, Ali SM, Kim DH, Guertin DA, Latek RR, Erdjument-Bromage H, et al. Rictor, a novel binding partner of mTOR, defines a rapamycin-insensitive and raptor-independent pathway that regulates the cytoskeleton. Curr Biol 2004;14:1296–302.
[10] Guertin DA, Stevens DM, Thoreen CC, Burds AA, Kalaany NY, Moffat J, et al. Ablation in mice of the mTORC components raptor, rictor, or mLST8 reveals that mTORC2 is required for signaling to Akt-FOXO and PKCalpha, but not S6K1. Dev Cell 2006;11:859–71.
[11] Sarbassov DD, Guertin DA, Ali SM, Sabatini DM. Phosphorylation and regulation of Akt/PKB by the rictor-mTOR complex. Science 2005;307:1098–101.
[12] Sahin F, Kannangai R, Adegbola O, Wang J, Su G, Torbenson M. mTOR and P70 S6 kinase expression in primary liver neoplasms. Clin Cancer Res 2004; 10:8421–5.
[13] Varma S, Khandelwal RL. Effects of rapamycin on cell proliferation and phosphorylation of mTOR and p70(S6K) in HepG2 and HepG2 cells over-expressing constitutively active Akt/PKB. Biochim Biophys Acta 2007; 1770:71–8.
[14] Parent R, Kolippakkam D, Booth G, Beretta L. Mammalian target of rapamycin activation impairs hepatocytic differentiation and targets genes moderating lipid homeostasis and hepatocellular growth. Cancer Res 2007;67:4337–45.
[15] Semela D, Piguet AC, Kolev M, Schmitter K, Hlushchuk R, Djonov V, et al. Vascular remodeling and antitumoral effects of mTOR inhibition in a rat model of hepatocellular carcinoma. J Hepatol 2007;46:840–8.
[16] Treiber G. mTOR inhibitors for hepatocellular cancer: a forward-moving target. Expert Rev Anticancer Ther 2009;9:247–61.
[17] Schulze-Bergkamen H, Fleischer B, Schuchmann M, Weber A, Weinmann A, Krammer PH, et al. Suppression of Mcl-1 via RNA interference sensitizes human hepatocellular carcinoma cells towards apoptosis induction. BMC Cancer 2006;6:232–45.
[18] Chen KC, Peng CC, Peng RY, Su CH, Chiang HS, Yan JH, et al. Unique formosan mushroom Antrodia camphorata differentially inhibits androgen-responsive LNCaP and -independent PC-3 prostate cancer cells. Nutr Cancer 2007;57:111–21.
[19] Peng CC, Chen KC, Peng RY, Chyau CC, Su CH, Hsieh-Li HM. Antrodia camphorata extract induces replicative senescence in superficial TCC, and inhibits the absolute migration capability in invasive bladder carcinoma cells. J Ethnopharmacol 2007;109:93–103.
[20] Yang HL, Chen CS, Chang WH, Lu FJ, Lai YC, Chen CC, et al. Growth inhibition and induction of apoptosis in MCF-7 breast cancer cells by Antrodia camphorata. Cancer Lett 2006;231:215–27.
[21] Shen YC, Wang YH, Chou YC, Chen CF, Lin LC, Chang TT, et al. Evaluation of the anti-inflammatory activity of zhankuic acids isolated from the fruiting bodies of Antrodia camphorata. Planta Med 2004;70:310–4.
[22] Hseu YC, Chang WC, Hseu YT, Lee CY, Yech YJ, Chen PC, et al. Protection of oxidative damage by aqueous extract from Antrodia camphorata mycelia in normal human erythrocytes. Life Sci 2002;71:469–82.
[23] Song TY, Yen GC. Protective effects of fermented filtrate from Antrodia camphorata in submerged culture against CCl4-induced hepatic toxicity in rats. J Agric Food Chem 2003;51:1571–7.
[24] Lee TH, Lee CK, Tsou WL, Liu SY, Kuo MT, Wen WC. A new cytotoxic agent from solid-state fermented mycelium of Antrodia camphorata. Planta Med 2007;73:1412–5.
[25] Liskay RM, Kornfeld B, Fullerton P, Evans R. Protein synthesis and the presence of absence of a measurable G1 in cultured Chinese hamster cells. J Cell Physiol 1980;104:461–7.
[26] van den Bogert C, van Kernebeek G, de Leij L, Kroon AM. Inhibition of mitochondrial protein synthesis leads to proliferation arrest in the G1-phase of the cell cycle. Cancer Lett 1986;32:41–51.
[27] Tsai SL, Suk FM, Wang CI, Liu DZ, Hou WC, Lin PJ, et al. Anti-tumor potential of 15,16-dihydrotanshinone I against breast adenocarcinoma through inducing G1 arrest and apoptosis. Biochem Pharmacol 2007;74: 1575–86.
[28] Herbert TP, Tee AR, Proud CG. The extracellular signal-regulated kinase pathway regulates the phosphorylation of 4E-BP1 at multiple sites. J Biol Chem 2002;277:11591–6.

[29] Chan AY, Dyck JR. Activation of AMP-activated protein kinase (AMPK) inhibits protein synthesis: a potential strategy to prevent the development of cardiac hypertrophy. Can J Physiol Pharmacol 2005;83:24–8.

[30] Ma L, Chen Z, Erdjument-Bromage H, Tempst P, Pandolfi PP. Phosphorylation and functional inactivation of TSC2 by Erk implications for tuberous sclerosis and cancer pathogenesis. Cell 2005;121:179–93.

[31] Nishida N, Fukuda Y, Komeda T, Kita R, Sando T, Furukawa M, et al. Amplification and overexpression of the cyclin D1 gene in aggressive human hepatocellular carcinoma. Cancer Res 1994;54:3107–10.

[32] el-Deiry WS, Nelkin BD, Celano P, Yen RW, Falco JP, Hamilton SR, et al. High expression of the DNA methyltransferase gene characterizes human neoplastic cells and progression stages of colon cancer. Proc Natl Acad Sci USA 1991;88:3470–4.

[33] Jung JK, Arora P, Pagano JS, Jang KL. Expression of DNA methyltransferase 1 is activated by hepatitis B virus X protein via a regulatory circuit involving the p16INK4a-cyclin D1-CDK 4/6-pRb-E2F1 pathway. Cancer Res 2007;67: 5771–8.

[34] Weng QP, Kozlowski M, Belham C, Zhang A, Comb MJ, Avruch J. Regulation of the p70 S6 kinase by phosphorylation in vivo. Analysis using site-specific anti-phosphopeptide antibodies. J Biol Chem 1998;273:16621–9.

[35] Pullen N, Thomas G. The modular phosphorylation and activation of p70s6k. FEBS Lett 1997;410:78–82.

[36] Lane HA, Fernandez A, Lamb NJ, Thomas G. p70s6k function is essential for G1 progression. Nature 1993;363:170–2.

[37] Raught B, Gingras AC. eIF4E activity is regulated at multiple levels. Int J Biochem Cell Biol 1999;31:43–57.

[38] Tam KH, Yang ZF, Lau CK, Lam CT, Pang RW, Poon RT. Inhibition of mTOR enhances chemosensitivity in hepatocellular carcinoma. Cancer Lett 2009;273:201–9.

[39] Memmott RM, Dennis PA. Akt-dependent and -independent mechanisms of mTOR regulation in cancer. Cell Signal 2009;21:656–64.

[40] Erdogan M, Pozzi A, Bhowmick N, Moses HL, Zent R. Signaling pathways regulating TC21-induced tumorigenesis. J Biol Chem 2007;282:27713–20.

[41] Hardie DG. The AMP-activated protein kinase pathway—new players upstream and downstream. J Cell Sci 2004;117:5479–87.

[42] Imamura K, Ogura T, Kishimoto A, Kaminishi M, Esumi H. Cell cycle regulation via p53 phosphorylation by a 5′-AMP activated protein kinase activator, 5-aminoimidazole-4-carboxamide-1-beta-D-ribofuranoside, in a human hepatocellular carcinoma cell line. Biochem Biophys Res Commun 2001;287: 562–7.

[43] Motoshima H, Goldstein BJ, Igata M, Araki E. AMPK and cell proliferation-AMPK as a therapeutic target for atherosclerosis and cancer. J Physiol 2006;574:63–71.

[44] Nagata D, Takeda R, Sata M, Satonaka H, Suzuki E, Nagano T, et al. AMP-activated protein kinase inhibits angiotensin II-stimulated vascular smooth muscle cell proliferation. Circulation 2004;110:444–51.

[45] Yin J, Gao Z, Liu D, Liu Z, Ye J. Berberine improves glucose metabolism through induction of glycolysis. Am J Physiol Endocrinol Metab 2008;294:E148–56.